Eur. Phys. J. E **19**, 251–262 (2006)
DOI 10.1140/epje/i2005-10049-y

THE EUROPEAN PHYSICAL JOURNAL E

The nucleosome: A transparent, slippery, sticky and yet stable DNA-protein complex

H. Schiessel[a]

Instituut-Lorentz, Universiteit Leiden, Postbus 9506, 2300 RA Leiden, The Netherlands

Received 4 August 2005 /
Published online: 2 February 2006 –

Abstract. Roughly three quarters of eucaryotic DNA are tightly wrapped onto protein cylinders organized in so-called nucleosomes. Despite this fact, the wrapped DNA cannot be inert since DNA is at the heart of many crucial life processes. We focus here on physical mechanisms that might allow nucleosomes to perform a great deal of such processes, specifically 1) on unwrapping fluctuations that give DNA-binding proteins access to the wrapped DNA portions without disrupting the nucleosome as a whole, 2) on corkscrew sliding along DNA and some implications and on 3) tail-bridging–induced attraction between nucleosomes as a means of controlling higher-order folding.

PACS. 87.16.Sr Chromosomes, histones – 87.15.He Dynamics and conformational changes

1 Introduction

The structure of the nucleosome core particle is known in exquisite detail from X-ray crystallography at 2.8 Å resolution [1] and recently at 1.9 Å [2]. The octamer is composed of two molecules each of the four core histone proteins H2A, H2B, H3 and H4. At physiological conditions stable oligomeric aggregates of the core histones are the H3-H4 tetramer (an aggregate of two H3 and two H4 proteins) and the H2A-H2B dimer; the octamer is then stable only if it is associated with DNA [3]. In the octamer the two dimers and the tetramer are put together in such a way that they form a cylinder with a ~ 65 Å diameter and a ~ 60 Å height. With grooves, ridges and binding sites the octamer defines the wrapping path of the DNA, a left-handed helical ramp of 1 and 3/4 turns, 147 bp length and a ~ 28 Å pitch. This aggregate has a twofold axis of symmetry (the dyad axis) that is perpendicular to the superhelix axis. A schematic view of the nucleosome core particle (NCP; the particle that is left when the non-adsorbed "linker" DNA is digested away) is given in Figure 1.

There are fourteen regions where the wrapped DNA contacts the octamer surface, documented in detail in reference [2]. These regions are located where the minor grooves of the right-handed DNA double helix face inwards towards the surface of the octamer. At each contact region there are several direct hydrogen bonds between histone proteins and the DNA sugar-phosphate backbone [1] as well as bridging water molecules [2]. In addition, there is also always a (cationic) arginine side chain extending into the DNA minor groove. A reliable quantitative estimate of the free energy of binding per sticking point is still missing.

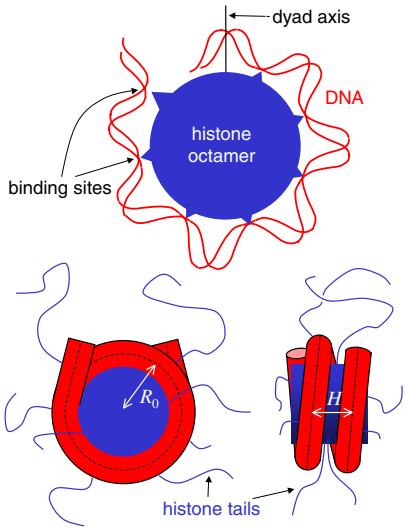

Fig. 1. Schematic views of the nucleosome core particle. The top picture displays only the upper half of the wrapped DNA with its binding points to the histone octamer (located at the positions where the minor groove faces the octamer). At the bottom the full NCP is shown from the top and from the side. Also indicated are the 8 histone tails.

An indirect method to estimate these values is based on studies of competitive protein binding to nucleosomal

[a] e-mail: schiessel@lorentz.leidenuniv.nl

DNA [4,5] that we will discuss in more detail in Section 2. From these experiments it can be estimated that the adsorption energy per sticking point is of order ~ 1.5–$2k_BT$, a number that —as we shall discuss in Section 2— has to be taken with caution. If we believe in this number for the moment, one should be aware of the fact that the 1.5–$2k_BT$ do not represent the *pure* adsorption energy but instead the *net* gain in energy that is left after the DNA has been bent around the octamer to make contact to the sticking point. A rough estimate of the deformation energy can be obtained by describing the DNA as a semiflexible chain with a persistence length l_P of $\sim 500\,\text{Å}$ [6]. Then the elastic energy [7] required to bend the 127 bp of DNA around the octamer (10 bp at each terminus are essentially straight [1]) is given by

$$\frac{E_{elastic}}{k_BT} = \frac{l_P l}{2R_0^2}\,. \tag{1}$$

Here l is the bent part of the wrapped DNA, $\sim 127 \times 3.4\,\text{Å} = 432\,\text{Å}$ and R_0 is the radius of curvature of the centerline of the wrapped DNA (cf. Fig. 1) that is roughly 43 Å [1]. This leads to a bending energy of order $58k_BT$, a number, however, that has again to be taken with caution since it is not clear whether equation (1) holds up to such strong curvatures. Especially, DNA does not bend uniformly around the octamer [8,9]. By using, nevertheless, these numbers, one can estimate the bending energy per ten basepairs, *i.e.*, per sticking site, to be of order $60k_BT/14 \sim 4k_BT$ [3].

Together with the observation that the net gain per sticking point is $\sim 2k_BT$ this means that the pure adsorption energy is on average $\sim 6k_BT$ per binding site. Note that the huge pure adsorption energy of $\sim 6k_BT \times 14 \sim 85k_BT$ per nucleosome is cancelled to a large extent by the $\sim 58k_BT$ from the DNA bending, a fact that has important consequences for nucleosomal dynamics.

Of great importance are also flexible, irregular tail regions of the core histones that make up $\sim 28\%$ of their sequences [10]. Each histone has a highly positively charged, flexible tail (the N-end of the polypeptide chain) that extends out of the nucleosome structure. Some of them exit between the two turns of the wrapped DNA, others on the top or bottom of the octameric cylinder. These N-tails are extremely basic due to a high amount of lysine and arginine aminoacids. They are sites of post-translational modification and are crucial for chromatin regulation. Especially, the tails have a strong influence on the higher-order structure of chromatin.

In this paper we focus on three physical mechanisms that might be of importance for the functioning of the nucleosome in the cell. In the next section we discuss unwrapping of DNA from nucleosomes. A theoretical interpretation of tension-induced unwrapping experiments suggests a mechanism by which the two-turn design allows the access of DNA binding proteins to nucleosomal DNA without disrupting the nucleosome as a whole, combining "transparence" and stability. Section 3 is devoted to possible mechanisms underlying nucleosome "sliding" along DNA. In Section 4 we discuss tail bridging as a possible mechanism for the attraction between nucleosomes. In the last section we provide discussions and conclusions.

2 How to combine transparence and stability

Consider a DNA fragment containing one nucleosome under an external force applied at the DNA termini. Clearly, for large enough forces the DNA unwraps from the octamer and the nucleosome falls apart. What is the critical force that is necessary to induce such an unwrapping? The answer seems to be straightforward: the length that is stored in the nucleosome is 50 nm and the net adsorption energy of these 50 nm amounts to $\approx 30k_BT$. Unwrapping the nucleosome means to release this wrapped length by paying the price of the net adsorption energy. The critical force should thus be

$$F_{crit} \approx \frac{30k_BT}{50\,\text{nm}} = 2.5\,\text{pN}. \tag{2}$$

The same critical force should be expected if there are several nucleosomes associated with the DNA fragment; all of them should unwrap at the same critical force. As turns out, the above-given line of reasoning is much too simple to capture the physics of the unwrapping process and, moreover, the numbers involved in equation (2) are most likely far off the real values.

A recently performed experiment [11] on a fiber of nucleosomes assembled from purified histones via salt dialysis made indeed observations that were very different from what equation (2) predicts (cf. also related experiments on native and reconstituted chromatin fibers [12–15]). The experiment was performed with a DNA chain with up to 17 nucleosomes complexed at well-defined positions (the DNA featuring tandemly repeated nucleosome positioning sequences). When small forces ($F < 10\,\text{pN}$) were applied for short times (~ 1–$10\,\text{s}$) the nucleosome unwrapped only partially by releasing the outer 60–70 bp of wrapped DNA in a gradual and equilibrium fashion. For higher forces ($F > 20\,\text{pN}$) nucleosomes showed a pronounced sudden non-equilibrium release behavior of the remaining 80 bp —the latter force being much larger than expected from the above-given equilibrium argument. To explain this peculiar finding Brower-Toland *et al.* [11] conjectured that there must be a barrier of $\sim 38k_BT$ in the adsorption energy located after the first 70–80 bp and smeared out over not more than 10 bp, which reflects some biochemical specificity of the nucleosome structure at that position. However, there is no experimental indication of such a huge specific barrier —neither from the crystal structure [2] nor from the equilibrium accessibility to nucleosomal DNA [4]. In reference [16] we argued that the barrier is caused by the underlying geometry and physics of the DNA spool rather than by a specific biochemistry of the nucleosome.

Our model [16] of a DNA spool under tension is shown on the top of Figure 2. We represent the DNA by a "Worm-Like Chain" (WLC) which provides a good description of the mechanical properties of the DNA [17].

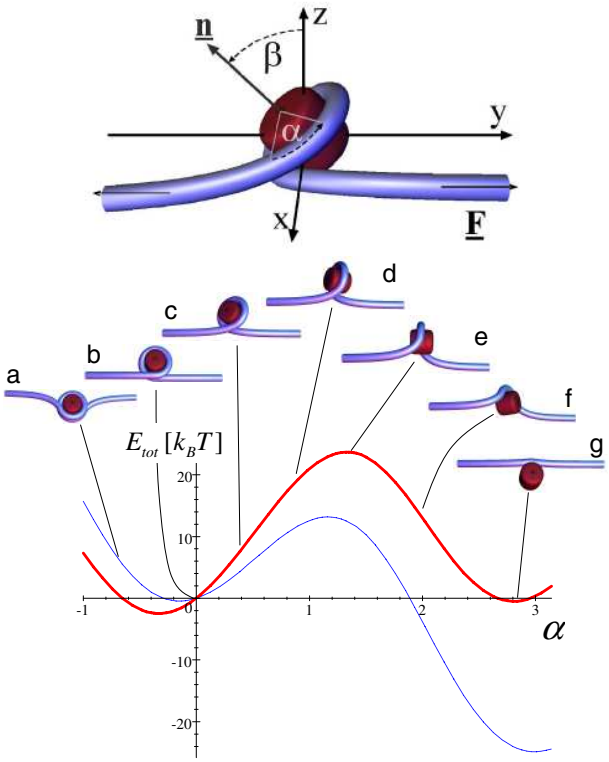

Fig. 2. A nucleosome under tension. The top picture defines the two angles involved in the unwrapping process: the desorption angle α and the tilting angle β. The bottom shows the nucleosome unwrapping that involves a 180° rotation of the octamer and the associated energy, equation (6), as a function of α for an applied tension of 6.5 pN. The thin curve represents a typical "traditional" estimate of adsorption energy density, $k^a = 2k_BT/\text{nm}$, where the applied force is far beyond the critical one. For the thick curve we choose $k^a = 3k_BT/\text{nm}$ — accounting for the first-second round difference [16]. In that case 6.5 pN corresponds to the critical force. Note that in both cases unwrapping is only possible as an activated process going across a substantial barrier.

The WLC is a semiflexible tube characterized by two moduli, the bending and the torsional stiffnesses. The torsional stiffness will be neglected in the following since we consider the case of freely rotating ends as in the experiments [11]. Then the elastic energy of a WLC of length L can be expressed as

$$E_{bend} = \frac{A}{2}\int_0^L \mathrm{d}s\kappa^2(s). \qquad (3)$$

Here A is the bending stiffness and $\kappa(s)$ the curvature of the chain at point s along its contour. The stiffness is related to the orientational persistence length l_P via $A = k_BTl_P$ (in fact, Eq. (1) is a special case of Eq. (3)). The DNA is assumed to be adsorbed on the protein spool surface along the predefined helical path with radius R_0 and pitch height H, cf. bottom of Figure 1, with a pure adsorption energy density per wrapped length, k^a, given by the pure attraction of the binding sites (not including the bending contribution).

The degree of DNA adsorption is described by the desorption angle α which is defined to be zero for one full turn wrapped (cf. top of Fig. 2). It is immediately clear that the unwrapping problem is non-planar and that the spool needs to rotate transiently out of the plane while performing a full turn —an effect already pointed out by Cui and Bustamante [12]. Therefore, a second angle, β, is introduced to describe the out-of-plane tilting of the spool, cf. Figure 2. When a tension F (along the Y-axis) acts on the two outgoing DNA "arms", the system (*i.e.*, the wrapped spool together with the free DNA ends) will simultaneously respond with DNA deformation, spool tilting and DNA desorption from the spool.

The total energy of the system as a function of α and β has three contributions:

$$E_{tot}(\alpha,\beta) = E_{bend} + 2R_0k^a\alpha - 2F\Delta y\,. \qquad (4)$$

The first term in equation (4) is the deformation energy of the DNA chain, equation (3), the second describes the desorption cost and the third term represents the potential energy gained by pulling out the DNA ends, each by a distance Δy.

It is possible to work out the total energy on purely analytical grounds by calculating the shape and energy of the DNA arms accounting for the right boundary conditions at the points where the DNA enters and leaves the spool and at the DNA termini (that are assumed to be far from the spool). Instead of giving the full analytical expression of E_{tot} (provided in Ref. [16]) we merely present here the limit for a flat spool with $R_0 \gg H$. In this case

$$E_{tot}\,(\alpha,\beta) = 2R\left[k^a - \frac{A}{2R_0^2} - F\right]\alpha + 2FR\cos\beta\sin\alpha + 8\sqrt{AF}\left[1-\sqrt{(1+\cos\alpha\cos\beta)/2}\right]. \qquad (5)$$

This is a good approximation for the nucleosomes where $R_0 = 4.3\,\text{nm}$ is larger than $H = 2.4\,\text{nm}$. In equation (5) the first term describes the competition between adsorption favoring the formation of the spool and the curvature of the wrapped portion and the external force, both trying to unwrap the DNA. The second term is a geometrical term that describes gain and loss of potential energy due to spool unwrapping (change in α) and rotation (change in β). The last and most important term accounts for the bending energy of the arms and cost of the potential energy due to the arms not being straight.

The energy landscape is mainly governed by that last term in equation (5). If we neglect the geometrical term (which one can easily check is a reasonable approximation) and go to the critical force at which the first term on the r.h.s. of equation (5) vanishes, $F_{crit} = k^a - A/(2R_0^2)$, then the transition path of the nucleosome is going along the line $\alpha = \beta$ from the minimum at $(\alpha,\beta) = (0,0)$ over the saddle point $(\pi/2,\pi/2)$ to another minimum of the same height at (π,π). The barrier height is given by $\Delta U \approx \Delta E_{tot} = 8\sqrt{AF}(1-1/\sqrt{2})$ and mainly stems from the strong bending of the DNA arms in the transition state, cf. configuration "e" in Figure 2.

This suggests —as a reasonable approximation— to set $\alpha = \beta$ in the full energy expression, equation (5):

$$E_{tot}(\alpha) \approx 2R\left[k^a - \frac{A}{2R_0^2} - F\right]\alpha + 2FR\cos\alpha\sin\alpha + 8\sqrt{AF}\left[1 - \sqrt{(1+\cos^2\alpha)/2}\right]. \quad (6)$$

In Figure 2 we plot the resulting energy landscape for a force of $F = 6.5\,\mathrm{pN}$. The thin curve corresponds to the value $k^a = 2k_BT/\mathrm{nm}$ as inferred from competitive protein binding data (see introduction); for the thick curve we assume a larger value, $k^a = 3k_BT/\mathrm{nm}$ (see below).

To compare our model to the unwrapping experiment [11] one needs to account for the fact that it was performed using dynamical force spectroscopy (DFS) [18]. The nucleosomal array was exposed to force F increasing at constant rate r_F, $F = r_F t$, and the most probable rupture force F^* as a function of loading rate was determined in a series of measurements. The rate of unwrapping is expected to be proportional to Kramers' rate [19] $\exp(\Delta U - \pi R(F_{crit} - F))$ from which it can be shown that $F^* \sim \ln(r_F) + \mathrm{const}$.

To our surprise, our detailed analysis showed that the rates over the barrier are much too fast in our model as compared to the rates at which nucleosomes unwrap in the experiment. This forced us to critically reconsider the assumptions on which the model was based, especially the —at first sight— straightforward assumption that the adsorption energy per length is constant along the wrapping path. But this neglects an important feature of the nucleosome, namely that the two DNA turns interact. Clearly the turns are close enough to feel a considerable electrostatic repulsion, the exact amount of which is hard to be determined, *e.g.* due to the fact that the DNA is adsorbed on the low-dielectric protein core (image effects). Moreover, the presence of histone tails complicates things. It is known (see Sect. 4) that the tails adsorb on the nucleosomal DNA. If the nucleosome is fully wrapped, the two turns have to share the cationic tails but if there is only one turn left, all these tails can in principle adsorb on this remaining turn. All these effects go in one direction: A remaining DNA turn on the wrapped nucleosome is much stronger adsorbed then a turn in the presence of the second turn wrapped. Indeed, very recent data by the same experimental group show that the force peaks of the discontinuous unwrapping events shift to substantially smaller values when the tails are partly removed or their charges partially neutralized [20].

The crucial point is now that the adsorption energy k^a was estimated from spontaneous unwrapping events of the second turn in the presence of the other turn [4,5] and thus k^a might have been strongly underestimated since the $k^a = 2.0k_BT/\mathrm{nm}$ include the unfavorable repulsion from the other turn. To account for this, we assumed that there is a different effective value of k^a for $\alpha > 0$ (less than one DNA turn) and for $\alpha < 0$ (more than one turn) [16]. Since the discontinuous unwrapping events observed in the experiment clearly correspond to the case where the last term is unwrapped (*i.e.* to the case $\alpha > 0$), we tuned the parameter k^a such that we can reproduce the DFS data in a satisfying way. From this we found that a value of $k^a = 3.0$–$3.5k_BT/\mathrm{nm}$ leads to a good agreement with the experimental data, a value that is *considerably* higher than the effective adsorption energy $k^a = 2k_BT/\mathrm{nm}$ felt when a turn is unpeeled in the presence of the other turn.

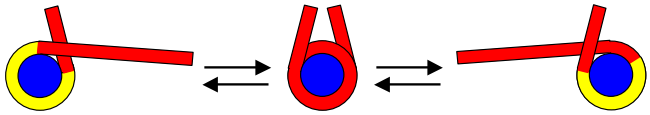

Fig. 3. (Colour on-line) The site exposure mechanism [4,5] allows the access to wrapped DNA via the spontaneous unravelling of DNA. Once only one turn is left (shown in yellow), this remaining turn has a strong grip on the octamer and further unpeeling becomes too costly (first-second round difference [16]; see text for details).

This result might explain how the nucleosome be transparent to DNA binding proteins and at the same time stable. When the nucleosome is fully wrapped each of the two turns can easily unwrap spontaneously due to thermal fluctuations and therefore all DNA is transiently accessible for DNA binding proteins, cf. Figure 3. This in fact has been proven experimentally via competitive protein binding by Widom and coworkers and has been termed the site exposure mechanism [4,5]; recently, fluorescence resonance energy transfer measurements has provided additional and more direct evidence for such conformational fluctuations [21,22]. What is, however, puzzling in this set of experiments is why the DNA stops to unpeel further once it encounters the dyad and why it does not fall apart. Our interpretation of the unwrapping data suggests that the reason for this is the first-second round difference. Once the DNA has unpeeled one turn, the remaining turn has a strong grip on the octamer since this turn does not feel the repulsion of the other turn.

3 How to slide along DNA and some immediate consequences

Another important mechanism is nucleosome "sliding". It has been observed under well-defined *in vitro* conditions that nucleosomes spontaneously reposition along DNA [23–26] transforming nucleosomal DNA into free DNA and *vice versa*. As turns out, heat-induced repositioning is a rather slow process happening on time scales of minutes to hours. The *in vivo* octamer repositioning has thus to be catalyzed by ATP consuming machines, so-called chromatin remodelling complexes [27,28].

Repositioning experiments (a detailed review is provided in Ref. [3]) have mostly been performed on short DNA fragments of lengths around 200 to 400 bp that contain one or two so-called positioning sequences. Repositioning is detected with the help of 2D gel electrophoresis making use of the fact that a complex with its octamer close to one of the DNA termini shows a higher electrophoretic mobility [23–25] than a complex where the

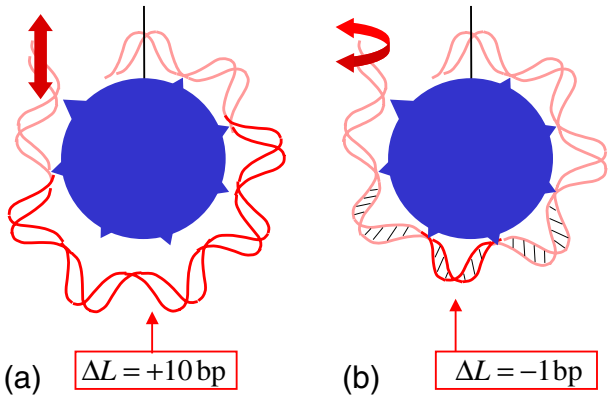

Fig. 4. Two possible mechanisms underlying the repositioning of nucleosomes: (a) bulge defects and (b) twist defects. Bulge defects contain typically an excess length of 10 bp leading to repositioning steps of 10 bp that in turn preserve the rotational positioning of the nucleosome. Twist defects carry either an extra or a missing basepair. This results in 1 bp repositioning steps and a concomitant corkscrew motion of the nucleosome.

octamer is located at the center of the DNA fragment. Another approach [26] makes use of a chemically modified histone protein that induces a cut on the nucleosomal DNA. What came out of these studies is that heat-induced repositioning is a slow process that takes place on the time scale of minutes to hours [23,26] at elevated temperatures (say 37°), whereas it is not observed at low temperatures like 5°. Another interesting feature is that the octamer is found at a preferred position (as mentioned above, the DNA contains a positioning sequence) or multiples of 10 bp, the DNA helical pitch, apart [23,26]; in addition, there is a preference for end positions [23]. On longer DNA fragments no evidence for a long-range repositioning has been found [24]. And finally, the presence of linker histones (H1 or H5) suppresses nucleosome mobility [25].

What causes nucleosome mobility? It is obvious that an ordinary sliding of the DNA on the protein spool is energetically too costly. As mentioned above, the interaction between the DNA and the octamer is localized at 14 binding sites, each contributing roughly $6k_BT$ pure adsorption energy [3]. A bulk sliding motion would involve the simultaneous breakage of these 14 point contacts, an event that would never occur spontaneously. As an alternative mechanism a rolling motion of the octamer along the DNA makes no sense: The helical wrapping path would simply cause the cylinder to roll off the DNA.

Repositioning must thus involve intermediates with a lower energetic penalty. The two possible mechanisms [3, 29] are based on small defects that spontaneously form in the wrapped DNA portion and propagate through the nucleosome: 10 bp bulges [30,31] (cf. Fig. 4(a)) and 1 bp twist defects [32] (cf. Fig. 4(b)). The basic idea of the bulge mechanism is as follows: First some DNA unpeels spontaneously from one of the termini of the wrapped portion [4,5]. Then that DNA is pulled in before it readsorbs creating an intranucleosomal DNA bulge that stores some extra length ΔL. This bulge diffuses along the wrapped DNA portion and finally leaves the nucleosome at either end. If the loop comes out at the end where it was formed, one is back at the original state. But if the loop leaves at the other end, the stored length ΔL has effectively been transported through the nucleosome and the octamer has moved by ΔL along the DNA. A careful quantitative analysis provided in reference [31] showed that the cheapest small loop has a length $\Delta L = 10$ bp, see Figure 4(a). Other loops are by far more expensive since they require twisting and/or stronger bending. But even a 10 bp loop is very expensive since its formation requires about $20k_BT$ desorption and bending energy. As a consequence the corresponding diffusion constant of the octamer along the DNA was found to be very small, namely on the order of $D \approx 10^{-16}\,\mathrm{cm}^2/\mathrm{s}$. Thus, typical repositioning times on a 200 bp DNA fragment are on the order of an hour, in reasonable agreement with the experimental data [23,26]. The strong temperature dependence and most strikingly the preference for 10 bp steps —corresponding to the extra length stored in the cheapest loops— is also in excellent agreement with the experiments. All these facts strongly vote for the loops as the mechanism underlying repositioning. There is, however, one serious caveat: We found that larger loops beyond one persistence length of DNA (roughly 150 bp) are easier to form than 10 bp bulges since such loops show a small curvature and have less desorbed binding sites [31]. Of course, for short DNA segments such loops cannot occur. But even in experiments with DNA segments of length ≈ 400 bp no signature of a long-range nucleosome repositioning has been found [24].

This observation led us to reconsider the underlying mechanism and to check whether nucleosome repositioning could be based on twist defects instead [32]. The basic idea is here that a twist defect forms spontaneously at either end of the wrapped DNA portion. Such a defect carries either a missing or an extra bp (Fig. 4(b) shows a missing bp). A defect is typically localized between two neighboring nucleosomal binding sites, *i.e.*, within one helical pitch (10 bp). This short DNA portion is stretched (compressed) and overtwisted (undertwisted). The energy of ± 1 bp twist defects was estimated from the combined stretch and twist elasticity of DNA including the (here unfavorable) twist-stretch coupling to be on the order of $9k_BT$ [32]. That means that —at a given time— one finds a twist defect only on one of around thousand nucleosomes.

Once a twist defect has formed, it diffuses through the wrapped DNA portion. The nucleosome provides between its 14 binding sites 13 positions for the defect. A defect —say a "hole" with a missing bp— moves from one position to the next in the fashion of an earthworm creep motion. The bp that is in contact with a binding site moves towards the defect resulting in an intermediate state where the defect is stretched out over 20 bp which lowers the elastic strain but costs desorption energy. Once the next bp has bound to the nucleosome, the twist defect has moved to the neighboring location. During this process the kink has to cross an energetic barrier on the order of $2k_BT$ [32]. Of course, not all twist defects that have formed will reach

the other end of the nucleosome, most fall off at the end at which they have been created. Assuming that all 13 possible defect locations are energetically equivalent, one can show that only 1/13 of the defects reach ultimately the other end and cause the nucleosomal mobility. Once such a twist defect has been released at the other end, the octamer makes a step by one bp *and* a rotation by 36° around the DNA axis; or *vice versa* one might say the DNA performs a corresponding corkscrew motion on the nucleosome.

Twist defects lead to a shorter step size of the octamer as compared to loop defects (1 bp *vs.* 10 bp) but this shorter length is dramatically overcompensated by their lower activation cost (roughly $9k_BT$ *vs.* $20k_BT$). In fact, putting all the above-given points together we were able to estimate the diffusion constant of the nucleosome along DNA to be $D_0 \approx 580\,\mathrm{bp}^2/\mathrm{s} \approx 7\times10^{-13}\,\mathrm{cm}^2/\mathrm{s}$ that is 3 to 4 orders of magnitude larger than the one predicted by loop defects [32]. The typical repositioning times on a 200 bp piece of DNA are thus predicted to be on the order of a second, a time much shorter than in the experiments. Also the predicted dependence of the dynamics on temperature is much too weak. Even worse, there is no "built-in" mechanism for 10 bp steps of the octamer. The experimentally observed preference for positions 10 bp apart manifesting itself in characteristic bands in the products of the gel electrophoresis [23,24] seems to be inconsistent with this mechanism —at least at first sight.

Here comes into a play an important additional feature of the repositioning experiments, namely that they are typically performed with DNA segments containing strong positioning sequences, especially the sea urchin 5S positioning element [23–25]. This sequence shows a highly anisotropic bendability of the DNA. If repositioning is based on twist defect, then the DNA has to bend in the course of a 10 bp shift in all directions, and thus has to go over a barrier. The elastic energy of the bent DNA is then a periodic function of the nucleosome position with the helical pitch being the period. We approximated this energy by an idealized potential of the form $U(l) = (A/2)\cos(2\pi l/10)$ with l being the bp number and A denoting the difference in elastic energy between the optimal and the worst rotational setting [32]. In principle, these oscillations die out completely when the nucleosome leaves the positioning sequence, *i.e.*, if it has moved around 140 bp. But since the templates are usually quite short (*e.g.* 216 bp [33]) the nucleosome always feels the rotational signal from the positioning sequence and our elastic energy should provide a reasonable description. As a result, the nucleosomal diffusion constant is reduced to the value [32]

$$D = \frac{D_0}{I_0^2\,(A/2k_BT)} \simeq \begin{cases} \frac{D_0}{1+A^2/8(k_BT)^2}, & \text{for } A < k_BT\,, \\ D_0\,\frac{\pi A}{k_BT}e^{-A/k_BT}, & \text{for } A \gg k_BT\,, \end{cases} \tag{7}$$

where I_0 is the modified Bessel function and D_0 denotes the diffusion constant for homogenously bendable DNA, $D_0 \approx 580\,\mathrm{bp}^2/\mathrm{s}$.

For the sea urchin 5S positioning element one has $A \approx 9k_BT$ [34,35] leading to a reduced mobility with $D \approx 2\times10^{-15}\,\mathrm{cm}^2/\mathrm{s}$. The typical repositioning times on a 200 bp DNA segment are now 2 to 3 orders of magnitude longer, *i.e.*, they are on the order of an hour —remarkably just as the ones in the loop case. It is now a simple matter of equilibrium thermodynamics that the probability of finding the DNA wrapped in its preferred bending direction is much higher than in an unfavorable direction. Thus, also in the case of 1 bp defects we expect to find nucleosomes mostly at the optimal position or 10, 20, 30, etc. bp apart corresponding to locations where still most of the positioning sequence is associated with the octamer and this in the preferred rotational setting. One would have to interpret then the bands in the gel electrophoresis experiments as a reflection of the Boltzmann distribution of the nucleosome positions rather than of the intrinsic step length. In other words, both the 10 bp bulge and the 1 bp twist defect lead in the presence of a rotational positioning sequences to pretty much the same prediction for the experimentally observed repositioning —even though the elementary motion is fundamentally different.

This leads to the question whether there are experimental data available from which the underlying mechanism can be induced. The most straightforward way would be to use a DNA template with less exotic mechanical properties. On an isotropically bendable DNA template nucleosomes mobility should not be affected if it relies on the loop mechanism but should be strongly enhanced for the twist defect case. The experiment by Flaus and Richmond [26] is in fact related to this idea. They measured repositioning rates on DNA fragments for two types of positioning sequences, namely nucleosome A on a 242 bp and nucleosome B on a 219 bp fragment, as a function of temperature. It was found that the repositioning rates depend strongly on temperature and on the positioning sequence: at 37 °C one has to wait $\sim$ 90 minutes for the A242 and more than 30 hours for the B219 for having half of the material repositioned. For the slower nucleosome B the sets of new positions were all multiples of 10 bp apart, *i.e.*, they all had the same rotational phase, whereas the faster nucleosome A did not show such a clear preference for a rotational positioning. It was argued that these differences reflect specific features of the underlying basepair sequences: Nucleosome B is complexed with a DNA sequence that has AA/AT/TA/TT dinucleotides with a 10 bp periodicity inducing a bend on the DNA, whereas nucleosome A is positioned via homonucleotide tracts. These observations are consistent with the twist defect picture where the corkscrew motion of nucleosome B is suppressed by the anisotropically bendable DNA template.

A different experimental approach was taken by Gottesfeld *et al.* [33]. The authors studied repositioning on a 216 bp DNA fragment that again contained the sea urchin 5S rDNA nucleosome positioning sequence but this time in the presence of pyrrole-imidazole polyamides, synthetic minor-groove binding DNA ligands, that are designed to bind to specific target sequences. Experiments have been performed in the presence of one of 4 different

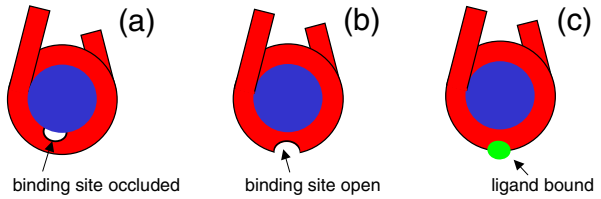

Fig. 5. Nucleosome repositioning in the presence of DNA ligands that bind at a specific site on the nucleosomal DNA. A nucleosome can then be in 3 different states, namely (a) with its ligand binding site occluded, (b) with its binding site open and (c) with a bound ligand. A nucleosome in state (c) cannot perform a corkscrew sliding.

ligands, each of which had one binding site on the nucleosomal DNA. It was found that a one-hour incubation at 37° in the absence of any ligand leads to a redistribution of the nucleosomes. This redistribution was completely suppressed in the presence of 100 nm ligands *if* the target sequence of this specific ligand faces outside (towards the solution) when the nucleosomal DNA is bent in its preferred direction. On the other hand, a ligand whose binding site faces the octamer in its preferred rotational frame had no detectable effect on the reposition dynamics.

Does the outcome of this experiment determine the mechanism underlying repositioning? Since the ligands bind into the minor groove (cf. the co-crystal complexes between nucleosomes and such ligands [36]), it is quite likely that a bound ligand will block the overall corkscrew motion of the DNA since the DNA can only rotate on the nucleosome up to a point where the bound ligand comes close to one of the 14 binding sites. That means that the observed suppression of mobility through ligand binding is consistent with the twist defect picture. But would it also be consistent with the bulge mechanism? The answer is in this case not obvious. But in a first approximation it seems plausible to assume that a bound ligand does not hinder bulge diffusion —at least sterically. A definite answer is hard since the ligand might locally alter the DNA elastic properties. But obviously the strong influence of ligand binding on nucleosome mobility supports the twist defect picture.

In reference [37] we determined the diffusion constant of a nucleosome along DNA in the various cases. In our model we assume that the nucleosome in the presence of a ligand can be in three states (cf. Fig. 5). Either the rotational setting of the wrapped DNA is such that its binding site is occluded (Fig. 5(a)) or it is facing the solution without a ligand (Fig. 5(b)) or with the ligand bound (Fig. 5(c)). Assuming thermodynamic equilibrium it is straightforward to determine the diffusion constant in the various cases. Especially we found for the case of a rotational position sequence with $A \gg k_BT$ in the presence of a ligand whose binding site is exposed in the preferred rotational frame

$$D = \frac{\pi A e^{-A/k_BT}}{k_BT} \frac{D_0}{1+K}, \tag{8}$$

whereas for the case of a ligand whose binding site is preferentially occluded we have

$$D = \frac{\pi A}{k_BT} \frac{D_0}{e^{A/k_BT}+K}. \tag{9}$$

Here $K = [L]/K_d$ is the equilibrium constant of the ligand of concentration $[L]$ and dissociation constant K_d. Obviously in the absence of ligands $K = 0$ and equations (8) and (9) reduce to equation (7) (for $A \gg 1$).

Equations (8) and (9) allow one to estimate the influence of ligands on repositioning in the various cases. In the following we define the typical equilibration time on a 216 bp long template (used in Ref. [33]) as $T_{70\,\mathrm{bp}} = (216-146)^2\,\mathrm{bp}^2/(2D)$. For an isotropic piece of DNA we estimated above $D = D_0 \approx 580\,\mathrm{bp}^2/\mathrm{s}$ leading to a typical equilibrium time $T_{70\,\mathrm{bp}} = 4\,\mathrm{s}$. If one uses a positioning sequence instead with $|\Delta G_{12}| = 9k_BT$ one finds in the absence of ligands from equation (7) $D \approx 2\,\mathrm{bp}^2/\mathrm{s}$ and $T_{70\,\mathrm{bp}} \approx 20\,\mathrm{min}$. Repositioning experiments on such sequences are thus typically performed on a time scale of an hour to ensure equilibration [23,33]. Adding now a ligand with $[L] = 100\,\mathrm{nM}$ and $K_d = 1\,\mathrm{nm}$ with a binding site that faces the solution in the preferred rotational frame we predict from equation (8) a dramatic reduction of the diffusion constant by a factor of 100: $D \approx 2\times10^{-2}\,\mathrm{bp}^2/\mathrm{s}$ and $T_{70\,\mathrm{bp}} \approx 34\,\mathrm{h}$. In this case one does not observe any repositioning of the nucleosomes on the time scale of an hour which is in accordance with the experimental observations, cf. Figure 5, lane 1 and 4 in the study by Gottesfeld *et al.* [33]. On the other hand, for the case of a ligand with the same affinity and concentration but with the binding site in the unfavorable orientation one finds hardly any effect; in fact the diffusion constant as compared to the ligand free case is reduced by approximately 1 percent, cf. equation (9). In the experiment [33] these two cases were indeed indistinguishable (cf. in Fig. 5, lane 0, 2 and 3 in that paper).

Additional experimental evidence for twist defect diffusion was provided in a recent study [38]. Edayathumangalam *et al.* analyzed polyamide binding to NCPs that contain either a 146 bp alpha satellite DNA sequence or a 147 bp version of the same sequence —with one additional bp at the dyad. For the latter sequence the two halves of the nucleosomal DNA have exactly the same rotational positioning with respect to the histone octamer, whereas there is a displacement by one bp between the two halves in the 146 bp NCP. Based on polyamide binding, DNase I and hydroxyl radical footprinting it was concluded that twist diffusion between different states does indeed occur in solution.

In conclusion, there is strong experimental evidence that autonomous repositioning of nucleosomes is based on twist defects. This process is slow in experiments since they are performed on DNA templates that contain nucleosome positioning sequences. However, only a small fraction of eukaryotic genomic DNA ($< 5\%$ [39]) seems to contain positioning sequences. This suggests a very dynamic picture of chromatin where the majority of nucleosomes are incessantly sliding along DNA —as long as they are not pinned to their location via linker histones [25].

Nucleosomal mobility has also profound consequences for the interaction of nucleosomes with motor proteins. Since most nucleosomes seem to be rather mobile, it might be that only positioned nucleosomes need the action of active (ATP consuming) remodelling mechanisms [40] making them switching elements bringing about, *e.g.*, gene activation or repression. Such chromatin remodelling complexes might catalyze the formation of twist defects or of bulges. In a recent experiment [41] it was found that a remodelling complex induced nucleosome repositioning even when the DNA was nicked and a torsion could not be transmitted —suggesting that at least for this specific example active repositioning might involve loop defects.

Finally, it is also tempting to speculate what happens when an RNA polymerase encounters a nucleosome. This should be a common event since tens to hundreds of nucleosomes are engaged with a given gene. There is a series of experiments [42–45] that report that RNA polymerase is capable to transcribe through nucleosomes. These are, however, highly artificial *in vitro* setups using bacteriophage RNA polymerase (never encountering nucleosomes in real life) performed on short DNA templates (*e.g.* 227 bp [42]) containing one nucleosome. The surprising finding of this set of experiments was that the polymerase can transcribe through the nucleosome and that as a product of this reaction one has a full-length transcript and the nucleosome at a new upstream position on the DNA template. To explain this remarkable result Studitsky *et al.* [42] suggested that the polymerase could cross the nucleosome in a loop (similar to the loop depicted in Fig. 4(a)) which would especially explain why the nucleosomes moves upstream. But this model is not consistent with the experiment by Gottesfeld *et al.* [33] who found that the polymerase gets stuck once it encounters a nucleosomes whose mobility is suppressed due to the presence of a minor-groove binding ligand (cf. Fig. 5(c)).

This observation led us to suggest an alternative mechanism that could explain the experimental findings [37]. We used our calculated nucleosomal mobilities to estimate that bacteriophage RNA polymerase should be typically strong enough to push a nucleosome in front of it in a corkscrew fashion —if the nucleosome is not pinned by a bound ligand. Furthermore, we put forward the idea that the octamer is not completely pushed off the DNA template but that the other free end (the one upstream) of the DNA recaptures the octamer. As a result, the octamer gets effectively transferred to an upstream position (cf. Fig. 3 in Ref. [37]). This would then suggest that transcription through nucleosomes is not such a straightforward task as suggested by the loop model. It is also consistent with the observation that transcription through a multinucleosomal DNA template leads under certain conditions to the destruction of the nucleosomal cores that the polymerase encountered on its way [46,47].

4 How to control the stickiness

Up to now we discussed single nucleosomes. In a cell, however, each DNA chain is complexed with millions of octamers distributed along the chain with a repeat length of roughly 200 bp [3]. A fiber with a 30 nm diameter, the chromatin fiber, is typically posited as the structure emerging from this string of nucleosomes [48]. In this fiber, and also in the higher-order structure beyond it, the nucleosome-nucleosome interaction plays a crucial role and this is the subject of the current section.

The chromatin fiber has a contour length that is about 40 times shorter than that of the DNA chain it is made from. But at the same time the fiber is much stiffer than the naked chain, so that its coil size in dilute solution would still be much larger than the diameter of the cell nucleus. Specifically, the size of a stiff polymer chain with persistence length l_P, diameter D and contour length L in a good solvent scales like $R \approx l_P^{1/5} D^{1/5} L^{3/5}$ [49]. A human chromosomal DNA chain has $L \approx 4\,\mathrm{cm}$. This together with $l_P = 50\,\mathrm{nm}$ and an effective diameter $D \approx 4\,\mathrm{nm}$ (assuming physiological ionic conditions) leads to $R \approx 100\,\mu\mathrm{m}$. On the other hand, the chromatin fiber has $L \approx 1\,\mathrm{mm}$, $l_P \approx 200\,\mathrm{nm}$ [50–52] and $D \approx 30\,\mathrm{nm}$ leading to $R \approx 20\,\mu\mathrm{m}$. There are 46 chains that have to fit into the nucleus with a diameter of 3 to $10\,\mu\mathrm{m}$. This clearly calls for the necessity of nucleosome-nucleosome attraction as a further means of compaction. This mechanism should be tunable such that fractions of the fiber are dense and transcriptionally passive, while others are more open and active.

This implies —among others— the following questions: Do nucleosomes attract each other and what is then the underlying mechanism? Can this interaction be tuned for individual nucleosomes? And can this be understood in simple physical terms? Recent experiments indeed point towards a simple mechanism for nucleosomal attraction: the histone tail bridging [53–55]. As mentioned in the introduction the histone tails are flexible extensions of the eight core proteins that carry several positively charged residues and whose lengths range from 15 residues (histone H2A) to 44 (H3). These tails extend considerably outside the globular part of the nucleosome as sketched schematically in Figure 1. Mangenot *et al.* [53] studied dilute solutions of NCPs. They demonstrated using small-angle X-ray scattering that NCPs change their size with salt concentration. At around 50 mM monovalent salt the radius of gyration increases slightly (from 43 Å to 45 Å), but at the same time the maximal extension of the particle increases significantly (from 140 Å to 160 Å). This was attributed to the desorption of the cationic histone tails from the NCP that carries an overall negative charge (cf. Ref. [3]). Osmometric measurements [54] detected around the salt concentration where the tails desorb an attractive contribution to the interaction between the NCPs, reflected in a considerable drop of the second virial coefficient. The coincidence of the ionic strengths for the two effects led Mangenot *et al.* to suggest that it is the tails that are mainly responsible for the attractive interaction, a picture supported by the fact that the attraction disappears once the tails are removed from the NCP [55].

On the theoretical side the role of histone tails is not clear. Attraction between simplified model nucleosomes has been reported [56,57], yet this model ignored the tails.

The nucleosome was modelled by a positively charged sphere and a semiflexible cationic chain wrapped around. The interaction between two such complexes (at zero temperature) showed an attraction at intermediate salt concentrations leading to a non-monotonic behavior of the second virial coefficient (cf. Fig. 4 in [56]). On the other hand, Podgornik [58] focused on tail bridging in a model where the NCP was represented by a point-like particle with an oppositely charged flexible chain. This system showed NCP-NCP attraction but there was no non-monotonic behavior of the second virial coefficient. Thus, the question arises whether it is really the tail bridging that causes the attraction between NCPs observed at intermediate salt concentrations.

Another possible mechanism for the attraction could be based on correlations between charged patches [59]. An example provides a recent computer simulation of Allahyarov *et al.* [60] who studied the interaction between spherical model proteins that carry charge patches; the second virial coefficient featured a non-monotonic behavior as a function of ionic strength. Also the non-monotonic interaction found by Boroudjerdi and Netz [56] can be interpreted to belong to this class of attraction induced by charge correlations.

Strong theoretical support that tails are important in the interaction of nucleosomes within a chromatin fiber comes from a very recent computer simulation [61] where the NCP crystal structure has been mimicked by a cylinder with 277 charge patches (accounting for charged groups on the surface of the NCP) with all the tails anchored to it. By switching on and off the charges on the tails it was found that the tails play a crucial role in the electrostatic nucleosome-nucleosome and nucleosome-linker DNA interaction within that chromatin fiber model —especially leading to a stabilization of the fiber at physiological salt conditions. Even though this study shows the importance of tails for the nucleosomal interaction, it does not reveal what is really the underlying physical mechanism.

In a recent study [62] we introduced a minimal model for an NCP with tails to test whether such a model shows attraction with a non-monotonically varying second virial coefficient, to demonstrate that this effect is qualitatively different from attraction through charge patches and that it can be used to facilitate control of the compaction state of chromatin. Our NCP model, termed the eight-tail colloid, consists of a sphere with eight attached polymer chains. The sphere is a very coarse-grained representation of the NCP without the tails, *i.e.*, the globular protein core with the DNA wrapped around. The sphere carries a central charge Z that represents the net charge of the DNA-octamer complex; since the DNA overcharges the cationic protein core, one has $Z < 0$ [3]. The eight histone tails are modelled by flexible, positively charged chains grafted onto the sphere. All parameters in the model have been chosen to match closely the values of the NCP. All charged monomers and the central sphere experience an electrostatic interaction via the standard Debye-Hückel (DH) interaction with an inverse screening length $\kappa = \sqrt{4\pi l_B c_s}$,

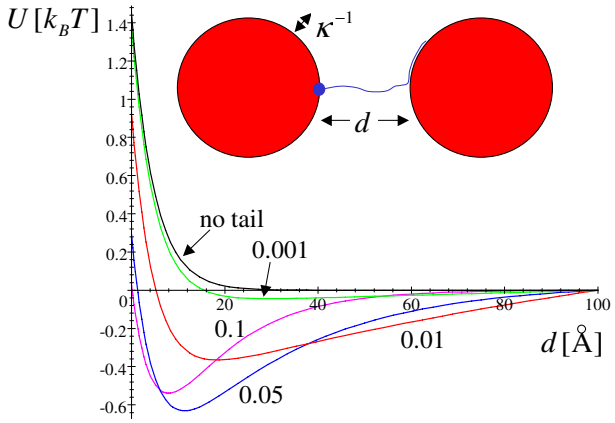

Fig. 6. Interaction potential, equation (13), for the interaction between two colloids in the presence of a tail. The parameters are chosen as follows: $l_B = 7$ Å, $Z = 50$, $\kappa = 0.2$ Å^{-1}, $R = 50$ Å and $l = 100$ Å. The numbers at the curves denote λ (in units of Å^{-1}).

where c_s denotes the monovalent salt concentration and $l_B = e^2/\epsilon k_B T$ (e: electron charge, ϵ: dielectric constant of the solvent) is the Bjerrum length.

We demonstrated via Molecular Dynamics simulation of a single eight-tail colloid that a single colloid shows similar features as the NCP, especially for small κ the tails are condensed onto the sphere and by increasing the screening the chains desorb and finally form random polymer coils [62]. We then determined the interaction between two such complexes. We found an attractive pair potential with a minimum of a few $k_B T$. The depth of the potential showed a non-monotonic dependence on κ which, in turn, was reflected in a non-monotonic dependence of the second virial coefficient A_2 with a minimum around the κ-value where the tails unfold. Again, all these observations are qualitatively similar to the experimental ones [54].

To determine whether this attraction can be attributed to the tail-bridging effect we compared the full eight-tail colloid to a simplified variant in which we collapsed each chain on a small patch modelled as a grafted monomer that carries the whole chain charge. Inspecting the attractive part of the pair potential we found that this patch model has a very rapidly decaying interaction with a characteristic length smaller than the screening length κ^{-1}. In sharp contrast, the eight-tail complex has a decay length that is considerably larger than κ^{-1}, an effect that can only be attributed to tail bridging.

In the following we put forward a simple theory for tail bridging. Consider two negatively charged colloids of radius R_0 and charge Z that represent two NCPs. Consider a positively charged chain of contour length l —end-grafted to one of the spheres as depicted in Figure 6— representing a tail. The line density of charges is $\lambda = f/b$ (b: monomer size, f: fraction of charged monomers) and d is the separation of the two colloid surfaces. Assume further the DH interaction of all charged components with screening length κ^{-1}. In the ground state the tail is adsorbed on the home core where each monomer feels the potential at

the sphere surface, $e\phi/k_BT = l_BZ/(\kappa R^2)$ (we drop here and in the following any numerical prefactors). Once the two balls are closer than the tail length, $d < l$, there is the possibility of forming a bridge. The cost of a bridge can be estimated from the number of monomers that are brought from the surface of the sphere to the region between the two balls where the potential is screened. These are $\approx \lambda(d-\kappa^{-1})$ monomers assuming that $d > \kappa^{-1}$. Hence the cost of the bridge is

$$\beta E_{bridge} = \left(d - \kappa^{-1}\right) \frac{l_B Z \lambda}{\kappa R^2}\,. \tag{10}$$

Two balls connected by a bridge feel the force

$$F = -\frac{\partial E_{bridge}}{\partial d} = -\frac{k_B T\, l_B Z \lambda}{\kappa R^2} \tag{11}$$

but a bridge only occurs with the probability $p_{bridge} = e^{-\beta E_{bridge}}$; otherwise there is no bridge and we assume no attractive contribution from the tail. The tail contribution to the potential of mean force is thus

$$\beta U_{bridge}(d) = -e^{-(d-\kappa^{-1})\frac{l_B Z\lambda}{\kappa R^2}} + e^{-(l-\kappa^{-1})\frac{l_B Z\lambda}{\kappa R^2}}\,. \tag{12}$$

To obtain the full potential we add the screened repulsion between the charged balls:

$$\beta U(d) = \frac{l_B Z^2}{(1+\kappa R)^2}\frac{e^{-\kappa d}}{d+2R} + \beta U_{bridge}(d). \tag{13}$$

We depict in Figure 6 the interaction potential, equation (13), for $l_B = 7\,\text{Å}$ (Bjerrum length in water at room temperature), $Z = 50$, $\kappa = 0.2\,\text{Å}^{-1}$, $R = 50\,\text{Å}$ and $l = 100\,\text{Å}$ for different values of λ, *i.e.* for different charge fractions of the tails (please note again that our estimate neglects numerical prefactors and we are here only focusing on qualitative and not on quantitative features). As can be seen from the curves the equilibrium distance goes to larger values and finally becomes extremely shallow when one goes from $\lambda = 0.1$ to $\lambda = 0.001$. Remarkably, this simple theoretical estimate produces curves that are qualitatively very similar to the ones obtained in our MD simulation of two interacting eight-tail colloids [62] where also the equilibrium distance goes to larger values and finally disappears.

We speculate now how the tail bridging can be used by the cellular machinery to control DNA compaction and genetic activity. It is in fact known that the cellular machinery is capable of controlling the charge state of the histone tails via the acetylation (the "discharging") and deacetylation (the "charging") of its lysine groups [63]. Active, acetylated regions in chromatin are more open; inactive, deacetylated regions tend to condense locally and on larger scales as well [64]. For instance, chromatin fibers tend to form hairpin configurations once a sufficiently strong internucleosomal attraction has been reached [52,65]. This suggests a biochemical means by which the degree of chromatin compaction and genetic activity can be controlled via a physical mechanism, the tail-bridging effect.

5 Discussion and conclusion

In this paper we have presented simple model representations of the nucleosome that allow to understand some of its physical properties. Modelling the nucleosome via a cylinder that exerts a short-range attraction to a semiflexible chain seems to be a reasonable representation when one wants to understand the unwrapping of the nucleosome under an externally imposed tension (that the attraction is caused by electrostatics is not of much importance here since the screening length is just 10 Å at physiological salt concentrations $c_s = 100\,\text{mM}$). During the unwrapping the nucleosome has to flip by 180° which leads to an energetically costly transition state with highly bent DNA portions. This can explain the dramatic rupture events observed in the experiments [11]. But even more: In order to explain the force spectroscopic data we were led to the conclusion that there must be a *first-second turn difference* [16] of the wrapped DNA portion as a result of an effective repulsion between the turns. This might explain why the *site exposure mechanism* [4,5] that allows transient access for DNA binding proteins to nucleosomal DNA does not lead to the complete disruption of the nucleosome: Thermal unwrapping stops once one turn is left on the nucleosome since that remaining turn has a firm grip on the octamer. In that way the two-turn design makes the nucleosome *transparent* to DNA binding proteins, yet assures its *stability*.

To describe *nucleosome sliding* along DNA one needs to use a more refined model of the nucleosome that takes into account the discrete binding sites between DNA and the octamer as well as the twist and stretch rigidity of the DNA [32]. This allows to understand the mobility of nucleosomes as being the result of small *twist defects* on the nucleosomal DNA that spontaneously form at the termini of the wrapped portion and that then propagate to the other end. That the nucleosomal mobility comes about via larger loops or bulges seems to be excluded from recent experimental data using synthetic DNA ligands [33]. A sliding nucleosome performs a corkscrew motion along the DNA, therefore probing, *e.g.*, the intrinsic curvature of DNA. That is why nucleosomes are substantially slowed down or even get stuck at nucleosome positioning sequences. Nucleosomal mobility might also be important when a transcribing RNA polymerase encounters nucleosomes [37]. Active repositioning is catalyzed via chromatin remodellers that in some cases might induce loop defects [41].

Finally, we focused on the role of the histone tails. To understand the basic physics of the attraction between nucleosome core particles (NCP) we suggest that it is —as a first step— sufficient to model them as negatively charged balls with positively charged tails attached [62]. This simple model is able to reproduce qualitatively several properties of NCPs such as the unfolding of the tails with increasing ionic strength [53] and the *attraction between NCPs* around the same ionic conditions [54]. The mechanism underlying this attraction is *tail bridging* where at least one tail of one NCP bridges to the other NCP. Since this tail bridging is strongly dependent on the charge state of the tail we speculate that acetylation of histone tails

reduces nucleosomal attraction so that acetylated chromosomal regions are more open and active.

Clearly it would be desirable to have a model of the nucleosome at hand that carries all the above-mentioned features at the same time. For instance, this might allow to estimate the role of histone tails in inducing the first-second round difference of the two DNA turns and in determining the dynamics of spontaneous DNA unwrapping. Having a grip on this dynamics it would be possible to check whether the opening fluctuations on the nucleosome have an impact on the repositioning rate via twist defects.

But much more important might be to develop a model that acknowledges the fact that the octamer is not just one unit but an aggregate of a H3-H4 tetramer and two H2A-H2B dimers. For instance, even around physiological ionic conditions the nucleosome might loose its dimers once the concentration of nucleosomes is too small. The recent study by Claudet *et al.* [15] shows, for instance, that the unwrapping data have to be taken with care. It is not always clear whether one unwraps an entire octamer from the DNA or whether under the given conditions there are mainly tetramers left. This might explain why the discrete unwrapping events correspond usually to the release of the last turn whereas there is no discrete unwrapping associated to the first turn. In fact, one might expect a double-flip unwrapping of the whole nucleosome, *i.e.*, two discrete peaks per nucleosome in the force-extension curve. We suggest, however, that the first peak is not visible since the corresponding DNA is much more weakly adsorbed (first-second round difference) and since in this case the height difference between entering and exiting DNA is much larger, which also considerably lowers the barrier against unwrapping of that turn. This issue certainly deserves more work on the experimental and theoretical side.

What is even more important: It is almost certain that the tripartite nature of the octamer is of importance for its functioning *in vivo*. Just to name one example: The "transcription through nucleosomes" discussed at the end of Section 3 leaves the nucleosome only intact for bacteriophage RNA polymerase but not for eucaryotic RNA polymerase II where the nucleosome looses one dimer [66]. Even though the use of short DNA templates might lead to serious artifacts —as we have pointed out above— this observation seems to suggest that eucaryotic RNA polymerase is prone to destroy the octamer and this might be important for its working *in vivo*.

A physical model of the nucleosome that —as simple as possible— takes the composite nature of the protein core into account might help to understand better how the nucleosome can manage to perform all its demanding tasks.

I have strongly benefitted from collaborations with Igor Kulić, Robijn Bruinsma, Bill Gelbart, Jon Widom, Frank Mühlbacher, Christian Holm, Farshid Mohammad-Rafiee, Boris Mergell and Ralf Everaers. I acknowledge fruitful discussions with John van Noort, Jan Bednar, Cyril Claudet, Stephanie Mangenot, Kurt Kremer, Rudi Podgornik, Jörg Langowski, Nikolay Korolev, Jordanka Zlatanova, Sanford Leuba and many others. I thank Joel Gottesfeld for sending reference [38] before publication.

References

1. K. Luger, A.W. Mäder, R.K. Richmond, D.F. Sargent, T.J. Richmond, Nature (London) **389**, 251 (1997).
2. C.A. Davey, D.F. Sargent, K. Luger, A.W. Maeder, T.J. Richmond, J. Mol. Biol. **319**, 1097 (2002).
3. H. Schiessel, J. Phys. Condens. Matter **15**, R699 (2003).
4. K.J. Polach, J. Widom, J. Mol. Biol. **254**, 130 (1995); **258**, 800 (1996).
5. J.D. Anderson, J. Widom, J. Mol. Biol. **296**, 979 (2000).
6. P.J. Hagerman, Annu. Rev. Biophys. Biophys. Chem. **17**, 265 (1988).
7. R.A. Harries, J.E. Hearst, J. Chem. Phys. **44**, 2595 (1966).
8. T.J. Richmond, C.A. Davey, Nature (London) **423**, 145 (2003).
9. F. Mohammad-Rafiee, R. Golestanian, Phys. Rev. Lett. **94**, 238102 (2005).
10. K. Luger, T.J. Richmond, Curr. Opin. Genet. Dev. **8**, 140 (1998).
11. B.D. Brower-Toland *et al.*, Proc. Natl. Acad. Sci. U.S.A. **99**, 1960 (2002).
12. Y. Cui, C. Bustamante, Proc. Natl. Acad. Sci. U.S.A. **97**, 127 (2002).
13. M.L. Bennink *et al.*, Nat. Struct. Biol. **8**, 606 (2001).
14. L.H. Pope *et al.*, Biophys. J. **88**, 3572 (2005).
15. C. Claudet, D. Angelov, P. Bouvet, S. Dimitrov, J. Bednar, J. Biol. Chem. **280**, 19958 (2005).
16. I.M. Kulić, H. Schiessel, Phys. Rev. Lett. **92**, 228101 (2004).
17. For reviews: M.D. Frank-Kamenetskii, Phys. Rep. **288**, 13 (1997); T. Schlick, Curr. Opin. Struct. Biol. **5**, 245 (1995).
18. E. Evans, K. Ritchie, Biophys J. **72**, 1541 (1997); E. Evans, Biophys. Chem. **82**, 83 (1999).
19. H.A. Kramers, Physica (Utrecht) **7**, 284 (1940).
20. B. Brower-Toland *et al.*, J. Mol. Biol. **346**, 135 (2005).
21. G. Li, M. Levitus, C. Bustamante, J. Widom, Nat. Struct. Mol. Biol. **12**, 46 (2005).
22. M. Tomschik, H. Zheng, K. van Holde, J. Zlatanova, S.H. Leuba, Proc. Natl. Acad. Sci. U.S.A. **102**, 3278 (2005).
23. S. Pennings, G. Meersseman, E.M. Bradbury, J. Mol. Biol. **220**, 101 (1991).
24. G. Meersseman, S. Pennings, E.M. Bradbury, EMBO J. **11**, 2951 (1992).
25. S. Pennings, G. Meersseman, E.M. Bradbury, Proc. Natl. Acad. Sci. U.S.A. **91**, 10275 (1994).
26. A. Flaus, T.J. Richmond, J. Mol. Biol. **275**, 427 (1998).
27. R.D. Kornberg, Y. Lorch, Cell **98**, 285 (1999).
28. P.B. Becker, EMBO J. **21**, 4749 (2002).
29. A. Flaus, T. Owen-Hughes, Biopolymers **68**, 563 (2003).
30. H. Schiessel, J. Widom, R.F. Bruinsma, W.M. Gelbart, Phys. Rev. Lett. **86**, 4414 (2001); **88**, 129902 (2002)(E).
31. I.M. Kulić, H. Schiessel, Biophys. J. **84**, 3197 (2003).
32. I.M. Kulić, H. Schiessel, Phys. Rev. Lett. **91**, 148103 (2003).
33. J.M. Gottesfeld, J.M. Belitsky, C. Melander, P.B. Dervan, K. Luger, J. Mol. Biol. **321**, 249 (2002).
34. C. Anselmi, G. Bocchinfuso, P. De Santis, M. Savino, A. Scipioni, Biophys. J. **79**, 601 (2000).

35. S. Mattei, B. Sampaolese, P. De Santis, M. Savino, Biophys. Chem. **97**, 173 (2002).
36. R.K. Suto, R.S. Edayathumangalam, C.L. White, C. Melander, J.M. Gottesfeld, P.B. Dervan, K. Luger, J. Mol. Biol. **326**, 371 (2003).
37. F. Mohammad-Rafiee, I.M. Kulić, H. Schiessel, J. Mol. Biol. **344**, 47 (2004).
38. R.S. Edayathumangalam, P. Weyermann, P.B. Dervan, J.M. Gottesfeld, K. Luger, J. Mol. Biol. **345**, 103 (2005).
39. P.T. Lowary, J. Widom, J. Mol. Biol. **276**, 19 (1998).
40. Y. Lorch, M. Zhang, R.D. Kornberg, Cell **96**, 389 (1999).
41. G. Längst, P.B. Becker, Mol. Cell **8** 1085 (2001).
42. V.M. Studitsky, D.J. Clark, G. Felsenfeld, Cell **76**, 371 (1994).
43. V.M. Studitsky, D.J. Clark, G. Felsenfeld, Cell **83**, 19 (1995).
44. V.M. Studitsky, G.A. Kassavetis, E.P. Geiduschek, G. Felsenfeld, Science **278**, 1960 (1997).
45. J. Bednar, V.M. Studitsky, S.A. Gregoryev, G. Felsenfeld, C.L. Woodcock, Mol. Cell **4**, 377 (1999).
46. B. ten Heggeler-Bodier, C. Schild-Poulter, S. Chapel, W. Wahli, EMBO J. **14**, 2561 (1995).
47. B. ten Heggeler-Bodier, S. Muller, M. Monestier, W. Wahli, J. Mol. Biol. **299**, 853 (2000).
48. B. Dorigo *et al.*, Science **306**, 1571 (2004).
49. T. Odijk, A.C. Houwaart, J. Polym. Sci. **16**, 627 (1978).
50. C. Münkel, J. Langowski, Phys. Rev. E **57**, 5888 (1998).
51. G. Wedemann, J. Langowski, Biophys. J. **82**, 2847 (2002).
52. B. Mergell, R. Everaers, H. Schiessel, Phys. Rev. E **70**, 011915 (2004).
53. S. Mangenot, A. Leforestier, P. Vachette, D. Durand, F. Livolant, Biophys. J. **82**, 345 (2002).
54. S. Mangenot, E. Raspaud, C. Tribet, L. Belloni, F. Livolant, Eur. Phys. J. E **7**, 221 (2002).
55. A. Bertin, A. Leforestier, D. Durand, F. Livolant, Biochemistry **43**, 4773 (2004).
56. H. Boroudjerdi, R.R. Netz, Europhys. Lett. **64**, 413 (2003).
57. H. Boroudjerdi, R.R. Netz, J. Phys. Condens. Matter **17**, S1137 (2005).
58. R. Podgornik, J. Chem. Phys. **118**, 11286 (2003).
59. I. Rouzina, V.A. Bloomfield, J. Phys. Chem. **100**, 9977 (1996).
60. E. Allahyarov, H. Löwen, J.P. Hansen, A.A. Louis, Phys. Rev. E **67**, 051404 (2003).
61. J. Sun, Q. Zhang, T. Schlick, Proc. Natl. Acad. Sci. U.S.A. **102**, 8180 (2005).
62. F. Mühlbacher, C. Holm, H. Schiessel, Europhys. Lett. **73**, 135 (2006).
63. P.J. Horn, C.L. Peterson, Science **297**, 1824 (2002).
64. C. Tse, T. Sera, A.P. Wolffe, J.C. Hansen, Mol. Cell. Biol. **18**, 4629 (1998).
65. S.A. Grigoryev, J. Bednar, C.L. Woodcock, J. Biol. Chem. **274**, 5626 (1999).
66. M.L. Kireeva *et al.*, Mol. Cell **9**, 541 (2002).